

Investigation of the boundary distortions in the presence of rotating external magnetic perturbations on ASDEX Upgrade

J. C. Fuchs¹, W. Suttrop¹, L. Barrera Orte¹, M. Cavedon¹, G. Birkenmeier¹, L. Giannone¹, L. Guimarais², A. Kirk³, B. Kurzan¹, P. J. McCarthy⁴, V. Nikolaeva², E. Wolfrum¹, E. Viezzer¹
and the ASDEX Upgrade Team¹

¹Max-Planck-Institut für Plasmaphysik, Garching, Germany

²Instituto de Plasmas e Fusão Nuclear, IST, Lisboa, Portugal

³CCFE, Culham Science Centre, Abingdon, UK

⁴Department of Physics, University College Cork, Ireland

Introduction

At ASDEX Upgrade non-axisymmetric magnetic perturbations produced by 16 in-vessel saddle coils have successfully been used to mitigate the plasma energy loss and peak divertor power load caused by Edge Localized Modes (ELMs), whereas concerning confinement and impurity concentration of both unperturbed ELM reference discharges and plasmas with mitigated ELMs show a similar behaviour [1]. The installed saddle coils allow magnetic perturbations with toroidal mode numbers up to $n=4$ and to vary the relative phase between the upper and lower rings. With the existing two power supplies slow rotating magnetic perturbation fields can be generated with mode numbers up to $n=2$, by exciting one of the power supplies

with a sine-shaped current and the other with a cosine-shaped current. Using subtle connections of the individual magnetic perturbation (MP) coils to the two power supplies, rotating perturbation fields with different phases between the upper and lower ring of MP coils are possible.

Influence of the finite coil geometry on the perturbation field

Ideally a perturbation field with mode number $n=2$ would vary smoothly toroidally with only an $n=2$ harmonic, and could also be rotated smoothly around the torus. However, in ASDEX Upgrade the eight MP coils of the lower ring extend over 45° each, and the coils of the upper ring over 37° with a gap of 8° between neighboured coils (figure 1). Because of the discreteness and almost rectangular shape of the coils sidebands and harmonics in the perturb-

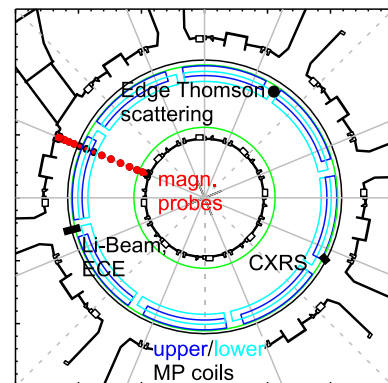


Figure 1: Toroidal view of ASDEX Upgrade with the position of the upper (dark blue) and lower (light blue) perturbation coils, separatrix position at the midplane (green), and some of the diagnostics used in this paper.

ation spectrum are created.

In order to investigate the influence of these imperfections on the plasma deformation, modeling of the separatrix displacement has been performed for the two extreme cases: One, where only every second MP coil is excited with the maximum coil current with alternating sign (figure 2, top), and the other, where pairs of neighboured MP coils are excited with $1/\sqrt{2}$ of the maximum coil current, again with alternating sign, which corresponds to a rotation of the perturbation field of half an MP coil, i.e. 22.5° (figure 2, bottom).

For these two configurations of MP coils, the separatrix displacement around the torus has been determined by using a field line tracing code to calculate the connection lengths to the outer and inner target [2], using the plasma magnetic field from the unperturbed equilibrium and the vacuum field of the perturbation coils [3]. The resulting separatrix displacements are compared in figure 3 for several z positions at the low field side. It is found that a significant effect of the coil geometry can only be seen directly in front of the MP coils (fig. 3a), whereas at the position of edge profile measurements the difference between the two configurations is either very small and within the error bars of the measurements (fig. 3b,d: at the height of the Li-beam or Doppler reflectometer measurements), or totally negligible (fig. 3c: at the midplane, which has the largest distance to both the upper and lower MP coils).

Influence of the rotating perturbation field on the boundary distortion

Several discharges have been performed with rotating perturbation fields, both in L- and H-

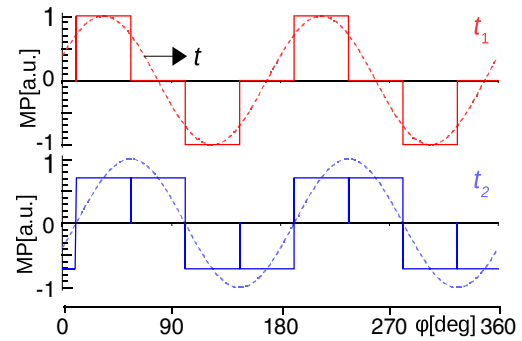


Figure 2: Ideal perturbation field (dashed) and approximation by finite MP coils (solid), showing the two extreme cases, where the bottom configuration is rotated by 22.5° (half an MP coil) against the top configuration.

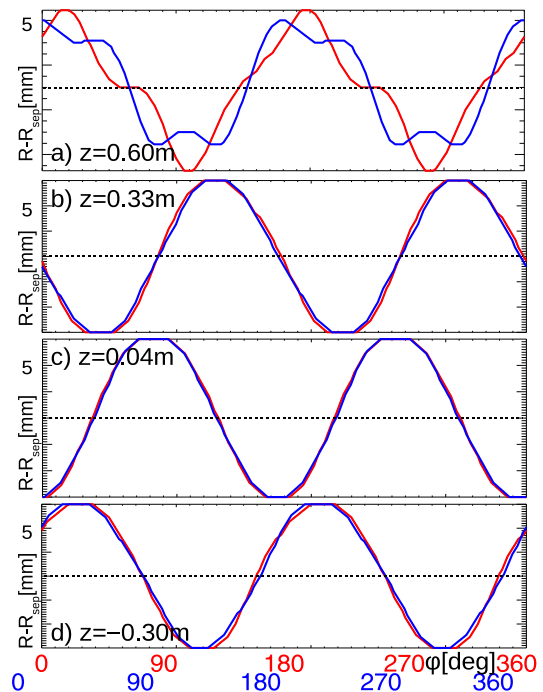


Figure 3: Calculated deformation of the separatrix at the low field side around the torus at four different z positions for the two cases from figure 2, where the curves for the second case (blue) have been shifted by 22.5° for easier comparison: a) directly in front of the upper MP coils ($z=0.60$ m), b) at the height of the Li beam diagnostic ($z=0.33$ m), c) at the height of the magnetic axis ($z=0.04$ m), d) at the height of the Doppler reflectometry measurements ($z=-0.30$ m).

mode, with both 2D equilibrium field-aligned (resonant) or non-field-aligned (non-resonant) phasings between the upper and lower coil sets. From the measurements of various edge profiles it can be seen that the plasma boundary is clearly affected by the perturbation field: Figure 4 shows that the distortion of various edge profiles is correlated to the phase of the applied perturbation field, for an H-mode shot with $B_T = -2.5$ T, $I_p = 0.8$ MA, $q_{95} = 5.2$, where the perturbation field has been rotated twice around the torus in 4 s (with 2 steps of NBI heating power of 5 MW and 7.5 MW). The fields from the upper and lower ring of coils were rotated in the same direction, with even parity ($\Delta\Phi = 0$) between the two rings, leading to a non-resonant configuration at the edge with the resonant field fraction of the applied perturbation, normalized to the toroidal field, of 0.06% at the edge. In the plasma core however ($\rho_{pol} < 0.8$) no similar influence of the perturbation field on the profile positions could be found from the measurements.

In order to check the measured profile variations at the edge with calculated boundary distortions, the perturbed separatrix position has been calculated as described above from the connection lengths to the outer and inner target. The displacements of the separatrix calculated with this vacuum field approach have been found to be consistent with those calculated by the NEMEC code [3]. Figure 5 shows the comparison of the calculated separatrix displacement with the distortion of the edge n_e profile measured by the Li-beam diagnostic for two shots: left the shot from figure 4, and on the right side a similar H-mode discharge, but where the fields from the upper and lower rings have been rotated in opposite directions, leading to both resonant and non-resonant phases at the edge (resonant field fractions between 0.04% and 0.15% at $\Psi_{nom} = 0.95$). In both discharges the line averaged density remained nearly constant, both in the edge and in the core, so that the changes in the density profiles are mainly due to the boundary displacement caused by the perturbation field. Separatrix displacements of ± 1 cm around the separatrix from the unperturbed, axisymmetric equilibrium are found (dashed line in fig. 5), and the variation of the density profile follows the separatrix displacement in both cases. Looking further inside the plasma however, in the first (non-resonant) shot

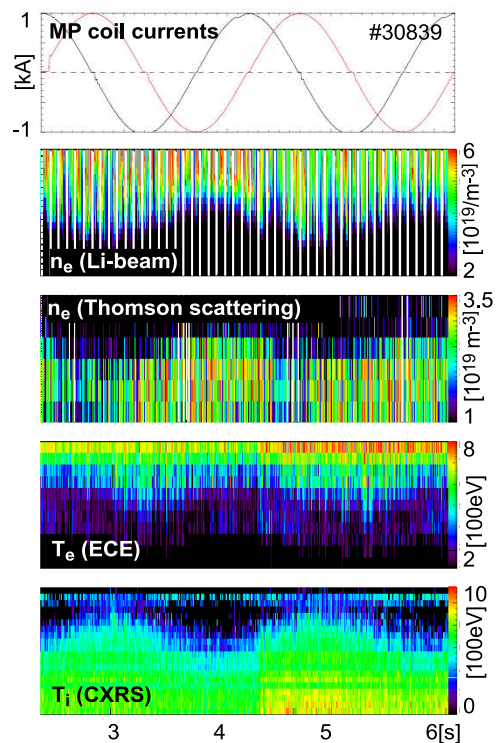


Figure 4: Distortion of edge profiles during a phase with a rotating perturbation field. Top: currents of the MP coils, below: contour plots of n_e , T_e and T_i at the edge. (The y-axis corresponds to different measurement channels of the particular diagnostic)

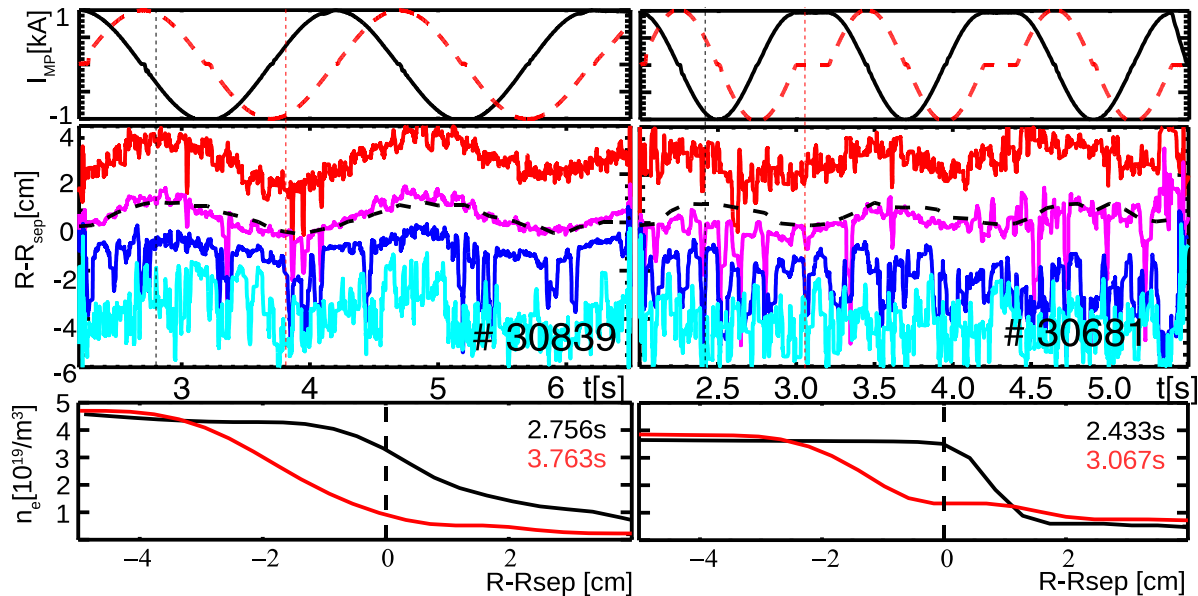


Figure 5: Comparison of the evaluation of edge density profiles, measured by the Li-beam diagnostic, with the perturbed separatrix position for two H-mode discharges.

Left: Perturbation field from the upper and lower set of MP coils is rotated in the same direction, even parity, non-resonant at the edge. Right: Perturbation field from the upper and lower set of MP coils is rotated in the opposite direction, both resonant and non-resonant phases.

Top: Currents of the MP coils. Middle: Contour lines of constant density (from 1 (red) to 4 (cyan) $\times 10^{19} \text{m}^{-3}$), as a function of time and the radial distance to the position of the separatrix from the unperturbed, axisymmetric equilibrium. The dashed black line denotes the position of the perturbed separatrix calculated with the vacuum field line approach. Bottom: density profiles as a function of the distance to the unperturbed separatrix for two time points with maximal inward or outward deformation of the perturbed separatrix.

the influence of the perturbation field can still be seen up to at least 3-4 cm inside the separatrix, whereas for the other (alternatively resonant and non-resonant) shot the influence of the perturbation field has almost disappeared in this region.

This leads also to a difference in the behaviour of the gradients of the n_e profiles, in the first case the density profile is mainly shifted around the separatrix of the unperturbed equilibrium, whereas in the second case it additionally flattens and steepens during the rotation of the perturbation field (figure 5, bottom). Similar behaviour is also found for other edge profiles and shot types, e.g. L-mode plasmas with different resonance conditions. This may lead to the assumption, that in non-resonant conditions the perturbation field may penetrate deeper into the plasma due to less shielding from the plasma, perhaps because of less plasma braking. This however still needs to be investigated with more detailed measurements and modeling of the penetration depth of the perturbation field.

References

- [1] W. Suttrop et al., *FED*, **88**, 446–453 (2013)
- [2] T. Eich et al, *Nucl. Fusion*, **40**, 1757 (2000)
- [3] J.C. Fuchs et al., EPS conference, **37D**, P4.126 (2013)
- [4] G. Conway et al, this conference, I4.115 (2014)

This project has received funding from the Euratom research and training programme 2014-2018